

# Cyclic AMP modifies the cellular distribution of connexin43 and induces a persistent increase in the junctional permeability of mouse mammary tumor cells

Michael M. Atkinson<sup>1,2,\*</sup>, Paul D. Lampe<sup>2,†</sup>, Helen H. Lin<sup>1</sup>, Rahn Kollander<sup>1</sup>, Xen-Ren Li<sup>1</sup> and David T. Kiang<sup>1</sup>

<sup>1</sup>Breast Cancer Research Laboratory, Division of Medical Oncology, Department of Medicine, University of Minnesota, Minneapolis, MN 55455, USA

<sup>2</sup>Department of Genetics and Cell Biology, University of Minnesota, 1445 Gortner Avenue, St Paul, MN 55018, USA

\*Author for correspondence at address 2

†Present address: Fred Hutchinson Cancer Research Center, Seattle, WA 98104, USA

## SUMMARY

Direct communication between cells via gap junctions is thought to be an important component of homeostasis and coordinated cellular responses to external signals. We investigated how the second messenger cAMP exerts its effects on junctional communication in a mouse mammary tumor cell line, MMT22. Junctional permeance was quantitatively assessed using dye microinjection and video microscopy. An increase of permeance was found after exposure to 8-bromo-cAMP, being detectable after 30 minutes of treatment and attaining a fourfold higher level of permeance by 24 hours. This elevated level was maintained with continuous exposure to 8-bromo-cAMP for seven days. The permeability change was accompanied by an increase in gap junctions as shown by freeze-fracture electron microscopy and by confocal microscopy using antibodies directed against the gap junction protein, connexin43. The amount of detergent-insoluble connexin43 also increased with 8-bromo-cAMP treatment, and most of

the increase could be attributed to an increase of slower migrating (i.e. phosphorylated) species of connexin43. However, connexin43 mRNA and the total cellular content of connexin43 did not change over this period of exposure to 8-bromo-cAMP, as shown by densitometric analyses of northern and western blots. We conclude that 8-bromo-cAMP affects the distribution of connexin43 such that a greater proportion of the protein is utilized for channel formation. Since these changes were relatively slow to develop and persisted with prolonged exposure to 8-bromo-cAMP, it is possible that the junctional permeability of these mammary tumor cells is linked to the 'basal' level of cAMP, i.e. levels maintained by the cells in accordance with a particular cell state.

Key words: cAMP, gap junction, permeability, connexin43, Cx43 mRNA, phosphorylation, quantitative videomicroscopy, mouse mammary tumor cell

## INTRODUCTION

Gap junctions are membrane structures featuring a variable number of aggregated intercellular channels that provide for direct cell-cell communication. A gap junctional hemi-channel from one cell is composed of hexameric connexin proteins that align in register with their counterparts in an opposing cell's membrane to form the intercellular channel. This arrangement provides a pathway for the flow of ions and small molecules (with dimensions under  $\approx 1.5$  nm) between cells (see reviews by Bennett et al., 1991; Beyer, 1993).

While it is difficult to ascribe a function to gap junctions without knowing the identities of the permeating molecules and the consequences of their passage to adjacent cells, the multiplicity of connexin species, their distribution in a wide variety of cells, and their differential expression over the lifetime of an organism suggest that gap junctions fulfill multiple purposes. One of these is likely the coordination of

various cellular responses, including proliferation and differentiation, effected by signal transfer through gap junctional channels (reviewed by Loewenstein, 1990). For example, numerous studies have shown a correlation between neoplastic transformation and some aberrant gap junctional feature, and it is frequently postulated that gap junctions may be critical to the control of cellular proliferation by providing for the spread of either positive or negative growth signals from cell to cell (Loewenstein and Rose, 1992; Sheridan, 1987; Trosko et al., 1990).

The classic signalling molecule, cAMP, has been shown to be important in the control of cellular proliferation (e.g. Cho-Chung, 1985) and in the control of gap junctional permeability (e.g. Azarnia et al., 1981; De Mello, 1984; Flagg-Newton et al., 1981; Mehta et al., 1992; Murray and Taylor, 1988; Saez et al., 1986), suggesting that the paths leading to growth regulation may converge. In a number of instances, an increase in cAMP has been correlated with reduced rates of cellular pro-

liferation (e.g. references in Cho-Chung, 1985), and an increase in junctional permeability (Mehta et al., 1992; Saez et al., 1986). Thus, cAMP may act to ensure adequate spread of the growth regulating molecule by increasing both the amount of the permeating molecule and the permeability of the cell-cell interface.

Because the permeability of gap junctions is governed by the number of functional channels as well as their individual gating properties, mechanisms for control of permeability may extend beyond gating to any one of several stages in the processes of intercellular channel formation or disassembly rates of synthesis and degradation of connexin mRNA (e.g. Mehta et al., 1992; Schiller et al., 1992), synthesis, transport, and oligomerization of connexins (e.g. Musil and Goodenough, 1991, 1993), requisite close apposition of adjacent cells (e.g. Keane et al., 1988), hemi-channel 'docking' across the intercellular space (e.g. Meyer et al., 1992), channel (or hemi-channel) aggregation (e.g. Preus et al., 1981), and perhaps removal of junctional plaques from the cell-cell interface (e.g. Saez et al., 1989). Deviations from normal processing at any of these stages could disrupt or reduce the normal functioning of gap junctions sufficiently to cause abnormal tissue growth.

Two recent studies have indicated that cAMP induces a large increase in connexin mRNA levels in different tumor cell lines and suggest that these increases account for the permeability changes induced by cAMP (Mehta et al., 1992; Schiller et al., 1992). Both studies show that the level of connexin43 (Cx43) mRNA and the degree of junctional coupling reached a peak and then decreased over time, even with continued elevation of cAMP. We report here on a fundamentally different form of control of junctional permeability by cAMP - one in which the cellular distribution of Cx43 is modified to elevate the gap junctional permeance without significant changes in Cx43 mRNA or the cellular allotment of Cx43 protein at the time permeability had attained maximal levels. Using a mouse mammary tumor cell line, we found that the increase in permeability with 8-bromo-cAMP (br-cAMP) treatment correlated with an increase in gap junctions, and that the cellular distribution of Cx43 shifted from a predominantly cytoplasmic membrane locale to gap junctional plaques at the cell surface. However, northern and western blot analyses of whole cell extracts showed that no increases were found for Cx43 message or protein. Prolonged exposure to br-cAMP maintained the high level of junctional permeability for several days with no evidence of a refractory period. The data are consistent with the concept that cAMP levels govern gap junctional permeability in these cells, and that, with persistent elevation of cAMP, a proportionately greater number of channels are maintained within junctional plaques at the expense of Cx43 storage pools elsewhere in the cell.

## MATERIALS AND METHODS

### Cell culture

MMT22 cells are mouse mammary tumor cells established from an hormonally-induced tumor (Kiang et al., 1982). Stock cultures were maintained in continuous passage using RPMI 1640 growth medium (Gibco) supplemented with 10% fetal bovine serum, 2 mM glutamine and antibiotics. Replicate plates were seeded using large aliquots from

a uniform suspension of well-dissociated cells to ensure equivalent plating densities. For experiments involving 7 days of exposure to 8-bromo-cAMP (br-cAMP; Sigma Chemical Co.), the cells were passed twice, and br-cAMP was replenished with each passage. The cell cultures were used two days after the last passage.

### Dye injection and analysis of permeance

Low density cultures of MMT22 cells in 60 mm culture dishes were grown for 24 to 48 hours before microinjection. The cultures were rinsed with phosphate buffered saline (PBS), mounted on the stage of an inverted fluorescence microscope, and microinjected with the fluorescent dye, Lucifer Yellow CH, as described previously (Atkinson and Sheridan, 1988). Analysis of dye spread between cell pairs was performed as described (Atkinson and Sheridan, 1988; Biegon et al., 1987) to derive a measure of the junctional permeance between pairs of cells. 'Permeance' refers to the property of gap junctional channels that supports diffusion of molecules under the driving force of a concentration gradient, akin to the property of conductance when ionic movement occurs under the driving force of an electric potential gradient. The permeance of a cell-cell interface is defined as the product of two terms: the permeability constant,  $P$ , of the aggregate junctional channels, and the total cross-sectional area,  $A$ , of the channels. The permeance of an interface between a cell pair can be calculated from measurements of the fluorescence intensity changes in the two cells over time ( $t$ ), and an estimate of the cell volumes ( $V_1$ ,  $V_2$ ). The linear equation describing this relationship is:

$$\ln(I_1 - I_1) = -PA \left( \frac{1}{V_1} + \frac{1}{V_2} \right) t + \ln I_0,$$

where  $I_1$  is the fluorescent intensity of the injected cell,  $I_2$  is the intensity of the dye-recipient cell, and  $I_0$  is the intensity in the injected cell at time zero. The slope of the line ( $-PA(1/V_1 + 1/V_2)$ ) can be used as a first approximation of permeance changes unless cell volumes vary substantially with the test condition. As can be seen from the equation, cell volume differences do not affect linearity; however, the volume of each cell in the pair affects the magnitude of the permeance. Rather than measure individual cell volumes, average cell volumes were used to estimate permeance. Cell volumes were calculated from diameter measurements of trypsinized (spherical) cells. Differences in sample thickness could be detected as a deviation from linearity. When this occurred, a correction was applied to the intensity values as described (Atkinson and Sheridan, 1988).

### Freeze-fracture electron microscopy

Cells were prepared for fracturing essentially as described (Atkinson et al., 1986). Replicas were scanned at 10,000-fold magnification for steps in the fracture plane indicative of a shift between E and P faces - transitions which are characteristic of opposed cells. These areas were sampled with a 3x3 array of fields at 30,000-fold magnification. Observations were restricted to areas including the membrane steps.

### Immunofluorescence staining

Cells were grown on acid-washed glass coverslips placed in a 35 mm tissue culture dish. For detergent-insoluble staining, cells were fixed in absolute ethanol for 10 minutes at room temperature, rinsed with PBS and incubated in PBS containing 0.2% Triton X-100, 5% BSA, and 0.02% sodium azide for 1-2 hours at room temperature. To visualize immunoreactive components in the detergent-soluble, cytoplasmic compartment, cells were fixed in acetone at  $-20^\circ\text{C}$  for 5-7 minutes, rinsed in PBS, and incubated in the above buffer without added Triton X-100. The cells were then rinsed and exposed to a mouse monoclonal antibody directed against the C terminus of Cx43 (Chemicon MAB 3068) or a mouse IgG (Sigma) which served as a control. Incubation was carried out in a humidified chamber at  $4^\circ\text{C}$  for 60 minutes. After several rinses, the cells were exposed to a rhodamine-tagged goat anti-mouse antibody (Cappel) for 30 minutes at  $4^\circ\text{C}$ , rinsed, and mounted onto glass slides.

### Confocal microscopy

Confocal microscopy was performed on a Bio-Rad MRC-600 equipped with a krypton/argon laser, Nikon Diaphot inverted microscope, Nikon  $\times 60$  Plan Apo objective (NA 1.4), and stage stepper motor. Images for each figure were collected under the same brightness and contrast settings using 1.5  $\mu\text{m}$ -2.0  $\mu\text{m}$  section thicknesses and an aperture setting that allowed some out-of-plane fluorescence to be imaged. Image analysis was performed on a personal computer (Macintosh Quadra, Apple Computer, Cupertino, CA) using the public domain software 'NIH Image' (available from the Internet by anonymous ftp from [zippy.nimh.nih.gov](http://zippy.nimh.nih.gov) or on floppy disk from NTIS, 5285 Port Royal Rd, Springfield, VA 22161, USA; part number PB93-504868).

### RNA analysis

Total cellular RNA was recovered from cell extracts (Chomczynski and Sacchi, 1987) following lysis. The RNA was separated by electrophoresis in a 2 M formaldehyde/1.5% agarose gel in 50 mM HEPES buffer, pH 7.8, containing 1 mM EDTA. RNA was transferred to a Biotrans nylon membrane (ICN Biomedicals, Inc.) and baked in a vacuum oven at 80°C for 1 hour. Hybridization was performed at 42°C overnight in a buffered solution containing 45% deionized formamide, 2 $\times$  SSC, 50 mM sodium phosphate, pH 6.5, 0.1% SDS, 5 $\times$  Denhardt's solution, 250  $\mu\text{g}/\text{ml}$  single-stranded calf thymus DNA, and 5 $\times 10^5$  cpm/ml of random-primed,  $^{32}\text{P}$ -labeled Cx43 probe. The nylon membrane was then washed four times in 2 $\times$  SSC, 0.1% SDS at room temperature for 5 minutes each, followed by two 15-minute washes in 0.1 $\times$  SSC, 0.1% SDS at 50°C. Autoradiography was performed with intensifying screens at -70°C for two days.

### Cx43 protein analysis

Cells grown in 60 mm dishes were lysed in the dish with a 2% SDS sample buffer containing 1  $\mu\text{g}/\text{ml}$  pepstatin A, 1  $\mu\text{g}/\text{ml}$  leupeptin, 1  $\mu\text{g}/\text{ml}$  aprotinin, and 2 mM phenylmethylsulfonyl fluoride (PMSF). After sonication in sample buffer, the samples were electrophoresed on SDS-polyacrylamide gels, following the method of Laemmli (1970), transferred to activated paper as previously described (Lampe and Johnson, 1990), and probed with an anti-Cx43 antibody (generously provided by Barbara Yancey; California Institute of Technology) generated against a synthetic peptide corresponding to the first 20 residues of the Cx43 N terminus (Yancey et al., 1989). Antigen/antibody binding complexes were exposed to 3  $\mu\text{Ci}$   $^{125}\text{I}$ -labeled Protein A (ICN), and the products visualized by exposure to Kodak XAR film overnight at -70°C with an intensifying screen. Use of the protease inhibitors reduced Cx43 proteolysis to undetectable levels indicated by an absence of lower molecular mass bands of approximately 30-35 kDa (detectable when using the N-terminal antibody (Laird and Revel, 1990); data not shown). Accurate protein determinations of the samples could not be obtained because of the protease inhibitors in the sample buffer. Consequently, the amount of material loaded in each lane was not based on equivalent protein; rather equivalent volumes were loaded and this typically resulted in equal Coomassie staining. If the loading appeared to be uneven in one or more lanes, all the samples were re-run using appropriate volumes to equalize Coomassie staining.

### Gel densitometry

Images of gels and autoradiographs were captured to disk with a Macintosh II microcomputer using a COHU CCD video camera, Fuji camera lens, and a frame grabber board (Data Translation, Inc.). Frame capture and densitometry were carried out using the NIH Image software described above. Band densities of the northern blots were obtained by measuring the area of a density profile curve for each band obtained from the Cx43,  $\alpha$ -actinin, or glyceraldehyde dehydrogenase (GAD) probes after background subtraction. Load variations were corrected by ratioing the band densities of Cx43 to GAD or to  $\alpha$ -actinin.

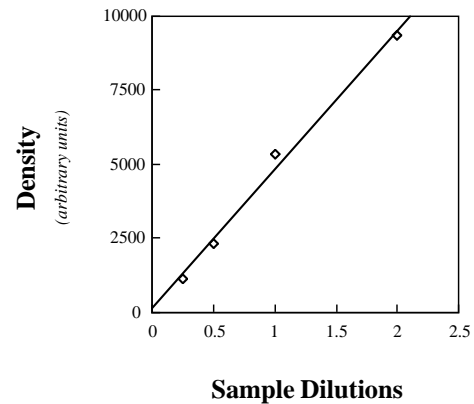


**Fig. 1.** Linearity of band density measurements in western blots with increasing sample load. The area (in arbitrary units) under the density profile curve were obtained from a serially diluted sample. The dilutions were run on a portion of the gel used in Fig. 8.

Band densities of each of the western immunoblots, obtained as described for the northern blots, were normalized to the appropriate band from 'control' (non-treated) samples and expressed as the fold change relative to control. Linearity of the densitometry measurements (correlation coefficient  $>0.98$ ) was confirmed by analyzing band densities obtained from a sample run at one-quarter, one-half, and twice the 'normal' protein load (Fig. 1). This indicated that the protein levels were below the saturation capacity of the paper, that the X-ray film band densities were proportional to load, and that the band densities were below the saturation level of the imaging equipment.

## RESULTS

### Permeance of cell-cell interfaces increased by br-cAMP

Quantitative analysis of the permeability of MMT22 cell interfaces to the junctionally-permeant dye, Lucifer Yellow CH, showed that increases were detectable after 30 minutes of exposure to 300  $\mu\text{M}$  br-cAMP, attained a fourfold increase by 24 hours, and maintained the high degree of cell-cell communication for 7 days (Fig. 2). The mean permeance of the cell-cell interfaces can be estimated from the individual slope values by factoring in the average cell volume (see equation in Materials and Methods). The average permeance for br-cAMP-treated cells was calculated to be  $5.9 \times 10^{-11}$   $\text{cm}^3/\text{second}$  ( $\pm 0.63$  s.e.m.) whereas the corresponding value for control cells was  $1.4 \times 10^{-11}$   $\text{cm}^3/\text{second}$  ( $\pm 0.24$  s.e.m.). This fourfold increase is highly significant ( $P < 0.0001$  by unpaired, two-tailed *t*-test). (Cells exposed to br-cAMP for 7 days had a somewhat greater average volume than control cells,  $1.53 \times 10^{-9}$   $\text{cm}^3$  ( $\pm 0.12$  s.e.m.) versus  $0.89 \times 10^{-9}$   $\text{cm}^3$  ( $\pm 0.06$  s.e.m.) for control cells). It should be noted that all of the junctional permeance data utilized cell pairs. Although not quantified, dye spread in confluent areas of the culture dishes also was increased with 6 hour, 24 hour, or 7 day exposure to br-cAMP (not shown).

### Number and size of gap junctions increased by br-cAMP

Freeze-fracture analysis was performed to determine if the increases in junctional permeance with br-cAMP treatment

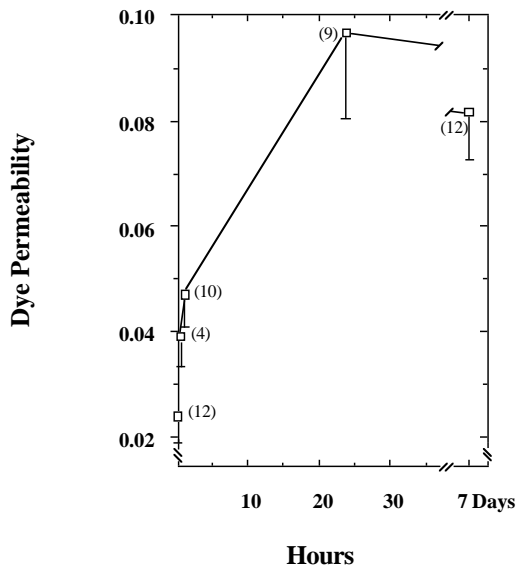


**Fig. 2.** Early changes in junctional permeability of MMT22 cells after addition of 300  $\mu$ M 8-bromo-cAMP are maintained for long periods with continuous exposure. Values for dye permeability (slopes of the lines generated from the equation shown in Materials and Methods) represent the change of dye concentration within the cell pair over time and are proportional to the permeance of the cell-cell interface. Numbers in parentheses next to each point show the number of cell pairs measured; error bars are s.e.m.

**Table 1. Gap junctional changes as determined by freeze-fracture analysis after a seven day exposure to 300  $\mu$ M br-cAMP**

	Control	br-cAMP
Total interfaces sampled	20	16
Positive interfaces found (% of total)	7 (35%)	10 (62.5%)
Total number of gap junctions	14	78*
Total number of gap junctional particles	847	8575*
Median number of particles per gap junction	25.5	33.5

\*Significantly different from control ( $P < 0.0001$ ) by Chi-Square analysis.

might be attributable to an increase in junctional plaques at cell-cell interfaces. As shown in Table 1, exposure of MMT22 cells to br-cAMP for 7 days resulted in an increased number of interfaces that contained gap junctions, and a large increase in the total number of gap junctions found, in the samples analyzed. Most of the increase occurred in the smaller gap junctions composed of less than 50 particles (Fig. 3). However, the number of gap junctions containing one hundred particles or more also increased ( $P < 0.02$ ; unpaired two-tailed  $t$ -test; see Fig. 3). These results indicate that the permeance increase found after seven days of exposure to br-cAMP parallel significant changes in the gap junctional plaques found at cell-cell interfaces, manifest predominantly as an increase in the number of gap junctions.

#### Cx43 immunostaining increases in parallel with permeability

The results of the dye transfer studies showed a gradual increase in transfer rates that plateaued by 24 hours of exposure

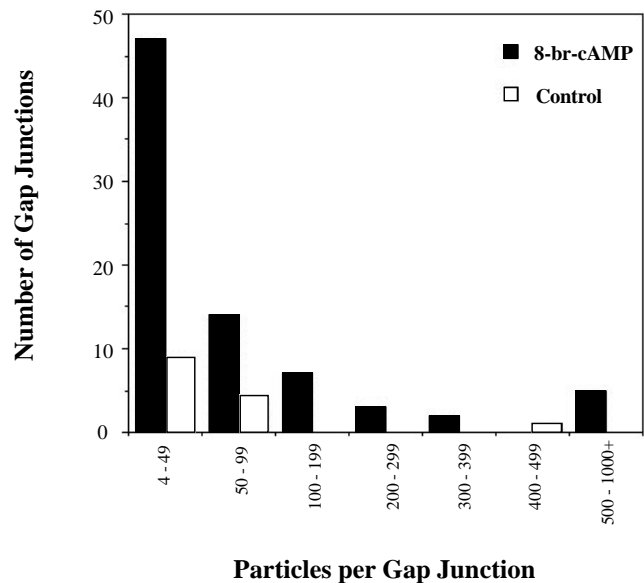


**Fig. 3.** Size distribution of gap junctions (number of particles/gap junction) in MMT22 cells revealed by freeze-fracture electron microscopy. Large increases in the number of small junctions (up to 100 particles/gap junction) were found after 7 days of treatment with 300  $\mu$ M br-cAMP, with an increase in the size of gap junctions also evident. Values are from two separate experiments.

to br-cAMP (cf. Fig. 2). Qualitatively similar results were obtained when MMT22 cells were immunostained for Cx43 after similar times of br-cAMP treatment (Fig. 4). Untreated MMT22 cells showed occasional punctate staining at cell-cell interfaces (Fig. 4A and Fig. 5), whereas cells exposed to br-cAMP for various times showed increasing amounts of interfacial staining (Fig. 4B-E and Fig. 6). The increase was manifest in the extent of interface stained and, frequently, in the size of the highly fluorescent puncta, perhaps corresponding to the increase in number and size of gap junctional plaques seen with freeze-fracture. Consecutive optical sections of control cells (Fig. 5) indicate that the punctate staining was confined to a few sections rather than widely distributed over the  $z$ -plane. This is also evident from optical sections of cells exposed to br-cAMP for six hours (Fig. 6).

Although Cx43 immunostaining showed an increase of punctate staining correlated with an increase of junctional permeability, the possibility remained that expression of a connexin other than Cx43 could also be contributing to the response, albeit to a small degree. However, northern analysis of control and br-cAMP-treated MMT22 cells (24 hour treatment) failed to reveal any transcript other than Cx43 mRNA when probed for Cx43, Cx40, Cx32, Cx31.1 and Cx26 (data not shown). Thus, while expression of another connexin has not been excluded completely, the data suggest that Cx43 is the salient connexin species.

#### The total cellular content of Cx43 mRNA and Cx43 protein was unchanged by br-cAMP treatment

The observed increased channel number and gap junctional permeability could have resulted from an elevated number of Cx43 transcripts, accelerated synthesis or decelerated removal of Cx43, and/or a change in the location of Cx43 from pre-

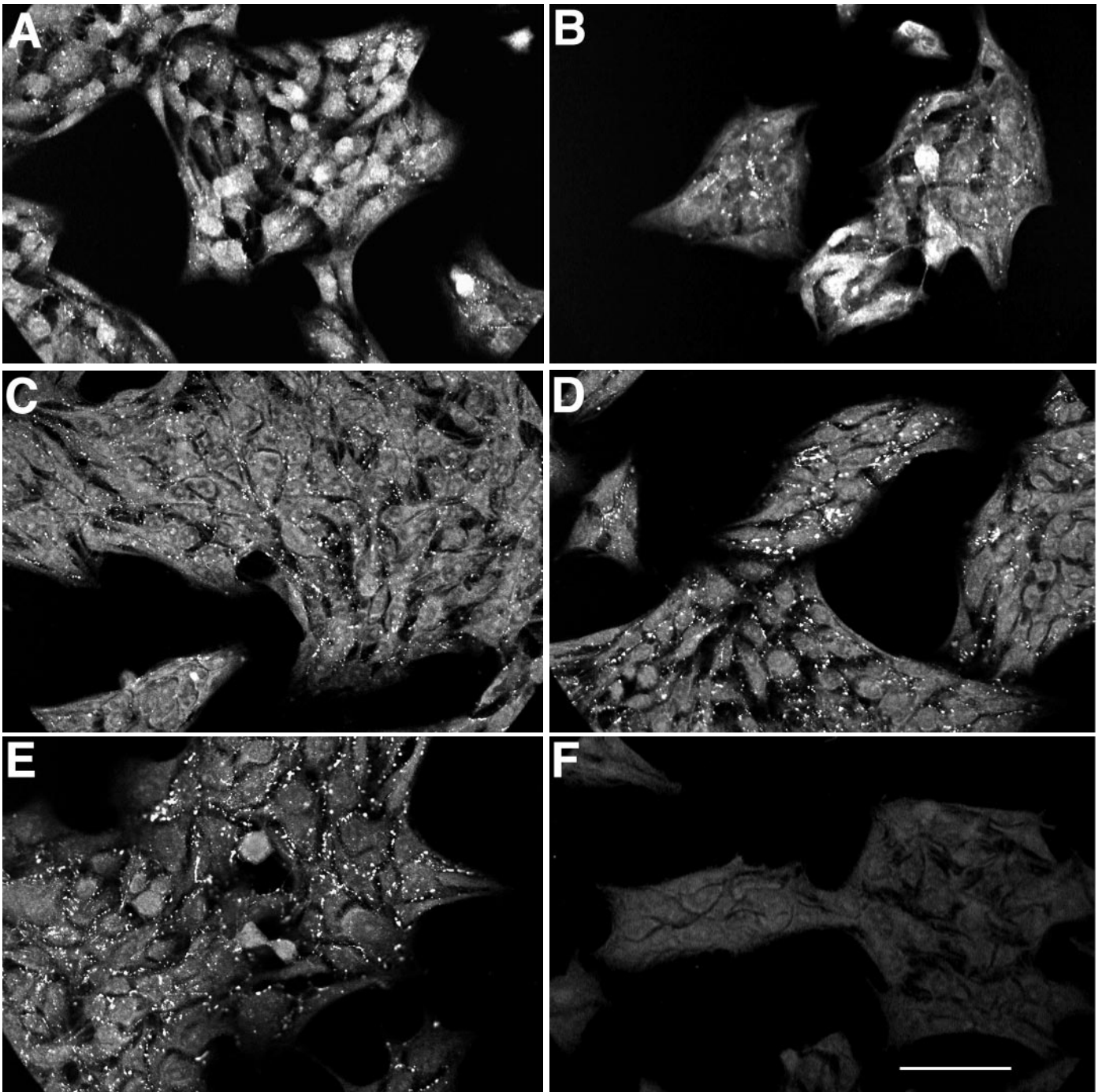


**Fig. 4.** Continuous exposure of MMT22 cells to br-cAMP increased the amount of gap junction protein at cell-cell interfaces as shown by immunofluorescence and confocal microscopy, using the mouse Cx43 monoclonal antibody. Each image is a single optical section of 1.5  $\mu\text{m}$  thickness. (A) Untreated control cells. (B-E) Time of exposure to 300  $\mu\text{M}$  br-cAMP. (B) 1 hour; (C) 6 hours; (D) 24 hours; and (E) 7 days. (F) Mouse IgG control. Bar, 50  $\mu\text{m}$ .

dominantly cytoplasmic or membrane storage sites to the junctional plaques. Northern and western blots were performed to determine whether the elevated amounts of Cx43 associated with the plasma membrane reflected an increase in the number of Cx43 transcripts and/or levels of total cellular Cx43 in response to br-cAMP, as had been reported by others (Mehta et al., 1992; Schiller et al., 1992).

Representative results from a northern analysis are shown in Fig. 7 and Table 2, which demonstrate that the level of Cx43 message essentially remained constant over the first 24 hours of exposure to br-cAMP. The small fluctuations in band densities were largely attributable to load variation, as shown by parallel changes in the amount of GAD and  $\beta$ -actin mRNA (Fig. 7 and Table 2; and by ethidium bromide staining - not

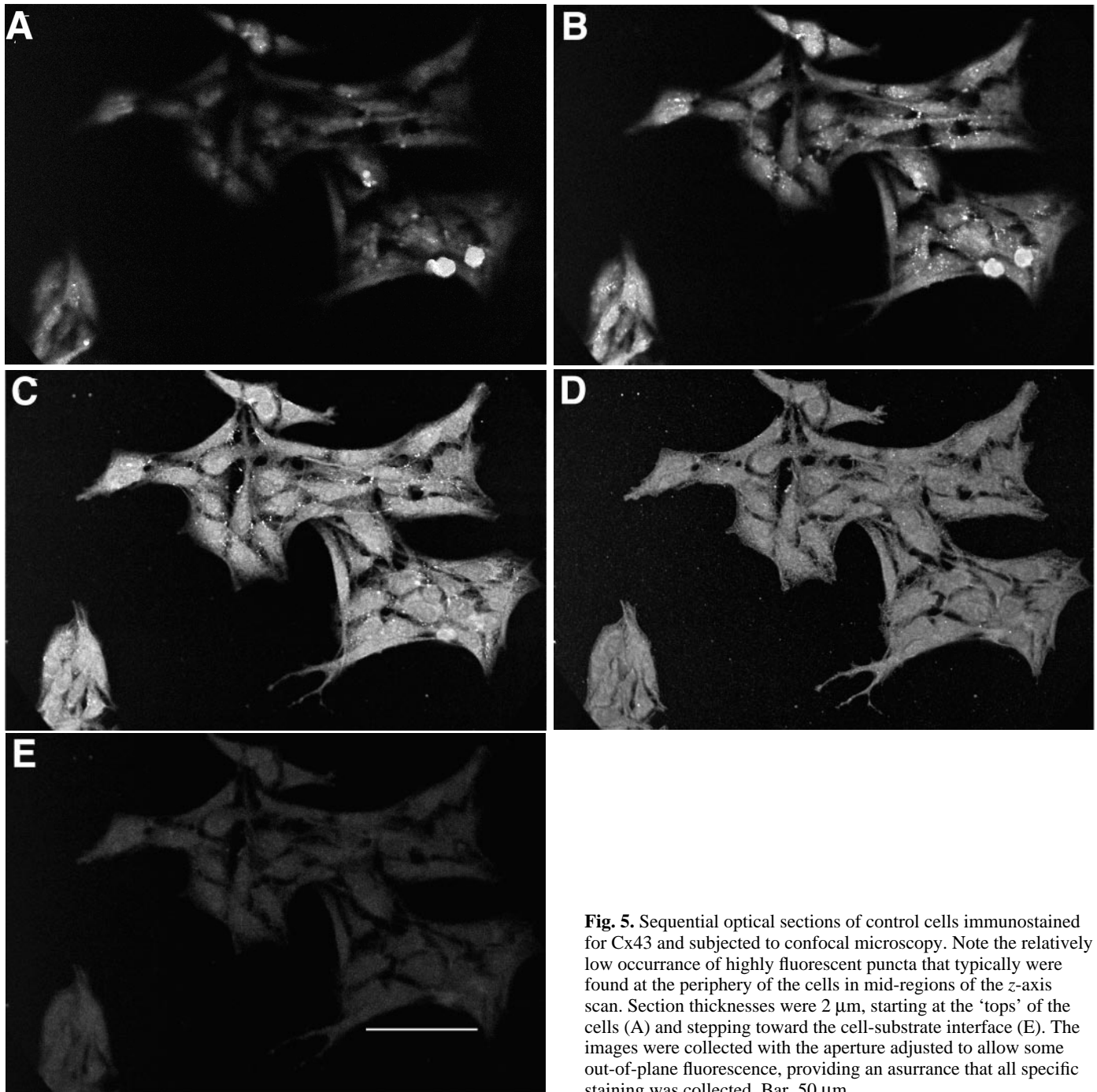


**Fig. 5.** Sequential optical sections of control cells immunostained for Cx43 and subjected to confocal microscopy. Note the relatively low occurrence of highly fluorescent puncta that typically were found at the periphery of the cells in mid-regions of the z-axis scan. Section thicknesses were 2  $\mu\text{m}$ , starting at the 'tops' of the cells (A) and stepping toward the cell-substrate interface (E). The images were collected with the aperture adjusted to allow some out-of-plane fluorescence, providing an assurance that all specific staining was collected. Bar, 50  $\mu\text{m}$ .

**Table 2. Densitometric analysis of Cx43 northern blot after varying times of 300  $\mu\text{M}$  br-cAMP treatment**

Time of br-cAMP exposure	Control	0.5 hour	1 hour	6 hour	24 hour	48 hour	7 day
Area of density profile* (fold change)							
Experiment 1	636 (1.0)	811 (1.3)	791 (1.2)	514 (0.8)	732 (1.2)	715 (1.1)	–
Experiment 2	705 (1.0)	–	623 (0.9)	541 (0.8)	–	949 (1.3)	978 (1.4)

\*Area measurements are expressed in arbitrary units. These values were corrected for load variation using measurements of GAD band densities. The same results were obtained using  $\beta$ -actin band densities (not shown).

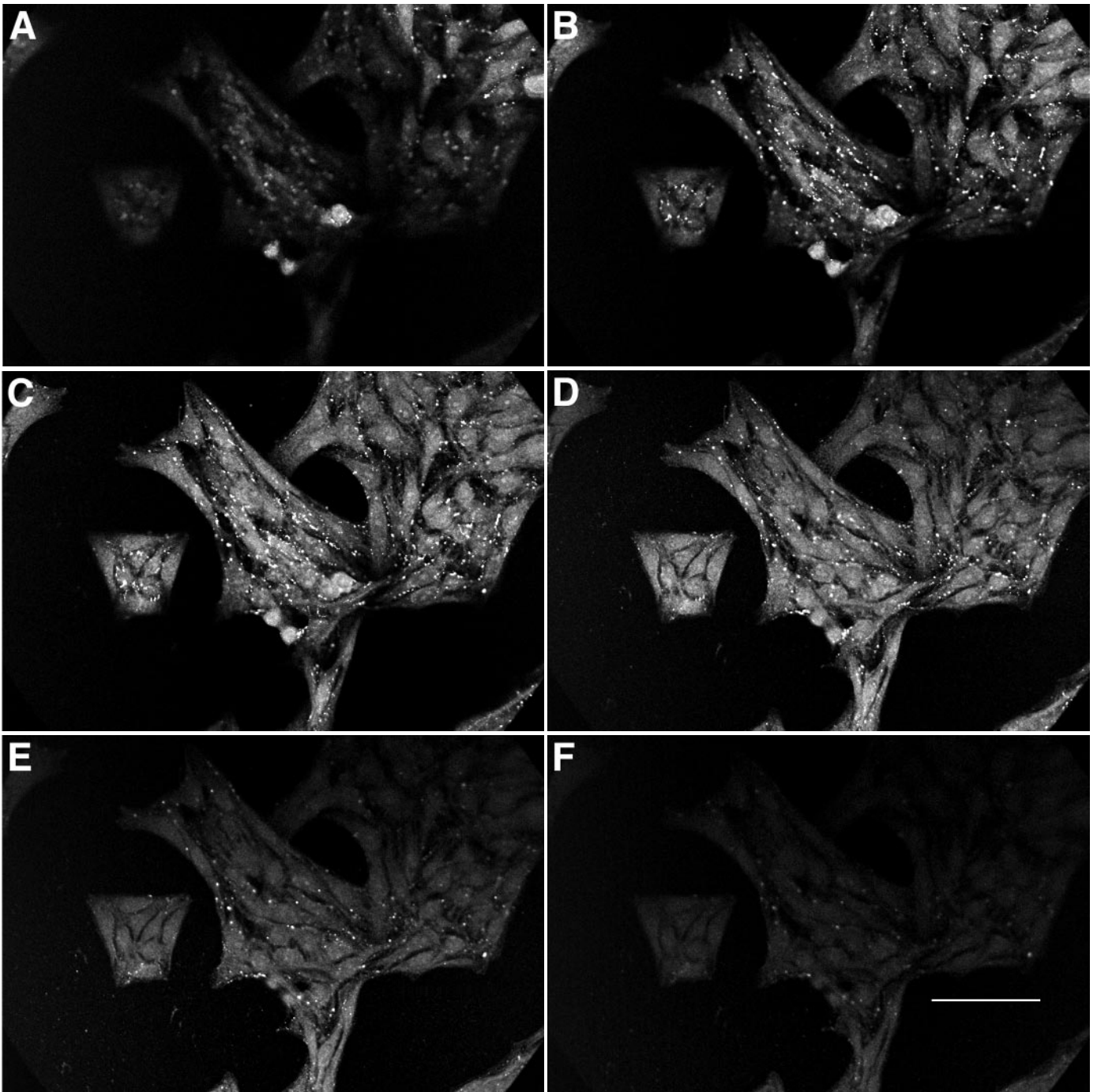


**Fig. 6.** Sequential optical sections of cells exposed to 300  $\mu$ M br-cAMP for 6 hours, immunostained for Cx43 and subjected to confocal microscopy. Contrast and brightness settings, and the aperture setting, were the same as for the control cells shown in Fig. 5. The section thicknesses were 1.5  $\mu$ m, starting at the 'tops' of the cells (A) and stepping toward the cell-substrate interface (F). Note the greater number of highly fluorescent puncta, relative to control, appearing at the periphery of the cells in mid-regions of the z-axis scan. (The z-plane was not orthogonal to the plane of the monolayer, causing a segregation of in-plane and out-of-plane fluorescence in each section.) Bar, 50  $\mu$ m.

shown). The modest increases in Cx43 mRNA relative to GAD and  $\beta$ -actin mRNA at the longer exposure times (Table 2) were observed in two of four additional assays (not shown).

While it is difficult to know whether the relatively small changes in Cx43 mRNA band density might be biologically relevant, any change in Cx43 message that has an impact on

the permeance of the cell-cell interface should also be manifest as a change in Cx43 protein levels. To assess this possibility, whole cell samples were immunoblotted for Cx43 after various times of exposure to br-cAMP. The western blot shown in Fig. 8 (which was run in parallel with the northern analysis shown in Fig. 7) is typical and shows a large and diffuse band of

**Table 3. Densitometric analysis of Cx43 western blot after varying times of 300  $\mu$ M br-cAMP treatment**

Time of br-cAMP exposure		Control	0.5 hour	1 hour	6 hour	24 hour	48 hour	7 day
Fold change of individual band densities								
Experiment 1	46 kDa	1.0	1.0	1.0	1.2	1.5	1.9	–
	44 kDa	1.0	0.9	1.2	0.8	1.0	0.9	–
	41 kDa	1.0	1.1	1.0	0.8	1.0	0.9	–
Experiment 2	46 kDa	1.0	–	1.0	1.2	1.6	2.7	3.3
	44 kDa	1.0	–	0.8	0.6	0.7	0.9	0.8
	41 kDa	1.0	–	0.9	0.7	0.9	1.2	0.9

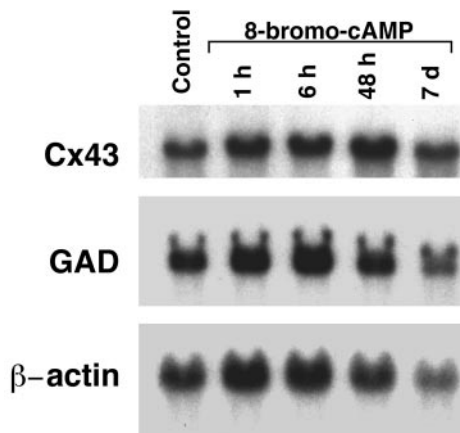


**Fig. 7.** The absence of large changes in Cx43 mRNA with br-cAMP treatment is indicated in this representative northern blot, showing Cx43 (top), GAD (center), and  $\beta$ -actin (bottom) mRNA from MMT22 cells exposed to 300  $\mu$ M br-cAMP for the times shown. Densitometry results for this blot (Experiment 2) are shown in Table 2.

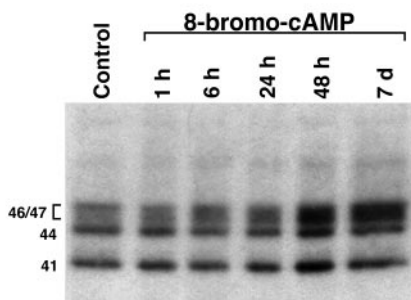


**Fig. 8.** The absence of large changes in Cx43 protein up to 24 hours of exposure to br-cAMP. This western was generated from the same cell preparation used for the northern blot in Fig. 7. Densitometry results for this immunoblot (Experiment 2) are shown in Table 3. Molecular mass (in kDa at left) was estimated from a standard curve.

approximately 46–47 kDa, a more distinct band of approximately 44 kDa, and a band of 41 kDa. In some instances, the 46/47 kDa band could be discerned as two distinct bands, but no attempt was made to distinguish these for the densitometry measurements. Several studies (e.g. Crow et al., 1990; Lau et al., 1992; Musil et al., 1990a,b), have shown that the lower (41 kDa) band is ‘non-phosphorylated’ Cx43, whereas the doublet band, and perhaps other, more slowly migrating species (Lau et al., 1992), are phosphorylated forms of Cx43. Consistent with this, immunoprecipitation of Cx43 in whole-cell extracts

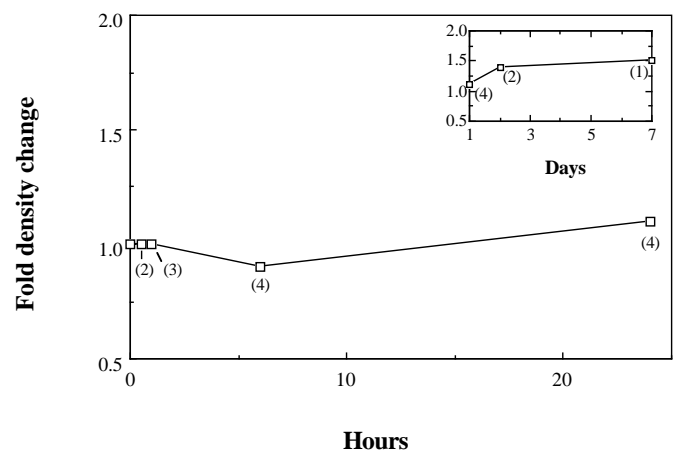


**Fig. 9.** No change in Cx43 levels, as measured by densitometry, was observed for br-cAMP exposure times up to 24 hours. Each point represents the fold change in total band densities (summation of the densities for 41 kDa, 44 kDa, and 46 kDa), as a measure of total Cx43, following exposure to 300  $\mu$ M br-cAMP for the times shown. Numbers in parentheses indicate the number of gels analyzed for each point. Inset: Expanded time course shows a 30%–50% increase in cellular Cx43 levels after 24 hours of exposure to br-cAMP.

from  $^{32}$ P-labeled MMT22 cells produced bands at 44–47 kDa on SDS-PAGE (not shown). Fig. 9 shows the densitometry results from 2 to 4 western blots for various time points of br-cAMP treatment up to 24 hours. Over this period, little or no change in total cellular Cx43 occurred. As shown in the inset of Fig. 9, a modest increase (30%–50%) in total cellular Cx43 was found for the two day and seven day time points.

Although the total cellular Cx43 levels are little affected by br-cAMP, a comparison of individual band densities indicates that the 46 kDa species progressively increased from the 6 hour time point onward, attaining 2- to 3-fold greater density relative to that obtained from the control cells (Table 3). Conversely, the 44 kDa band and the 41 kDa band were either unchanged or slightly reduced in density.

These findings make it unlikely that increased Cx43 synthesis or depressed Cx43 degradation account for the permeability changes during the first 24 hours of br-cAMP treatment, by which time the maximal fourfold increase in permeance had been obtained. Moreover, the modest increase in total Cx43 after 24 hours of br-cAMP exposure falls short of the fourfold or greater increase in gap junctional channels suggested by measurements of permeance (cf. Fig. 2). Instead, the data indicate a translocation of pre-existing Cx43 from non-junctional stores to junctional plaques and suggest that some phosphorylation of Cx43 accompanies the transition.

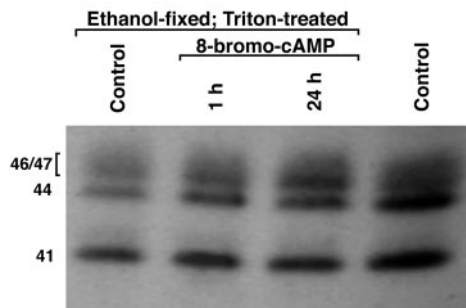


**Fig. 10.** Detergent-extraction reveals an increase in detergent-insoluble Cx43 as shown by western blot analysis. Cells were fixed in ethanol and extracted with Triton X-100 as per the immunofluorescence protocol. Material run in the far right lane was obtained from cells handled as for Fig. 4 (lysed immediately with sample buffer; see Materials and Methods) Densitometry results are shown in Table 4 (Experiment 1). Molecular masses (in kDa) are shown at the left.

### Detergent-insoluble forms of Cx43 increased after 1 hour of br-cAMP treatment

The western data from whole cell extracts seemed to contradict the immunofluorescence data (cf. Figs 4,5,6), which clearly showed increased immunostaining with time of exposure to br-cAMP and predominant if not exclusive localization of Cx43 at the periphery of the br-cAMP-treated cells. However, the use of detergent to permeabilize the cells may have depleted the non-junctional stores of Cx43 (e.g. Musil and Goodenough, 1991). Therefore, we processed MMT22 cells exactly as was done for the immunostaining (ethanol fix and detergent permeabilization) and ran western blots on the material remaining attached to the dishes to determine if Cx43 on western blots would now show an increase in parallel with the increase in Cx43 immunostaining. In addition, the blots primarily should reflect the characteristics of plasma membrane-associated Cx43.

As shown in Fig. 10, total (detergent-insoluble) Cx43 appeared to progressively increase with exposures to br-cAMP for 1 hour and 24 hours. Densitometry data from two experiments (summarized in Table 4) indicated that the increase in Cx43 predominantly was due to an increase in density of the 46 kDa and 44 kDa bands, while the amount of the 41 kDa species did not appreciably change. Interestingly, both of the

**Table 4. Densitometric analysis of Cx43 western blot from ethanol-fixed and detergent permeabilized cells after 300  $\mu$ M br-cAMP treatment**

Time of br-cAMP exposure		Control	1 hour	24 hour
Fold change of Cx43				
Experiment 1		1.0	1.5	1.8
Experiment 2		1.0	1.4	1.7
Fold change of individual bands				
Experiment 1	46 kDa	1.0	1.7	2.4
	44 kDa	1.0	1.7	1.8
	41 kDa	1.0	1.2	1.2
Experiment 2	46 kDa	1.0	2.0	2.3
	44 kDa	1.0	2.3	3.0
	41 kDa	1.0	1.0	1.0

presumably phosphorylated species showed an increase of approximately twofold after only 1 hour of br-cAMP treatment.

### Distribution of Cx43 cytoplasmic immunostaining to Cx43 plasma membrane immunostaining altered after exposure to br-cAMP

If ethanol fixation and detergent permeabilization does extract non-junctional Cx43, as seemed to be the case, it would be useful to determine the immunostaining pattern of Cx43 in the absence of detergent. Therefore, control and br-cAMP-treated cells were fixed and permeabilized in acetone (acetone was used to allow for non-detergent permeabilization) and processed for immunofluorescence as described in Materials and Methods. As shown in Fig. 11, cells not exposed to br-cAMP revealed an immunofluorescence pattern dominated by diffuse cytoplasmic patches of relatively low fluorescence intensity (Fig. 11A), whereas cells exposed to br-cAMP for 24 hours appeared to contain relatively large, highly fluorescent puncta at the cells' periphery and less conspicuous cytoplasmic labeling (Fig. 11B). Image analysis was performed to assess the intensity, number, and area of regions in Fig. 11A,B with the attribute of being highly fluorescent. In this case, highly fluorescent was defined as areas within the intensity range of 1 to 100 (arbitrary units on a scale of 1 to 255, brightest to darkest). As shown in Table 5, cells treated for 24 hours with br-cAMP displayed a greater number of such regions and consequently a higher total area of bright regions (approximately a threefold increase in both categories). Mean and median areas were unchanged in the treated cells. Note that the number of cells analyzed in each image is comparable (70 control cells and 69 treated cells) so that the values can be directly compared. Analysis was also performed on Fig. 11A,B to characterize the intensity, number, and area of the diffuse cytoplasmic patches. Regions displaying intensity values within the range of 101 to 200 and an area greater than  $\approx 4.3 \mu\text{m}^2$  were selected for analysis (Table 6). In this case, the number of regions falling within these parameters were the same for control and treated cells.

**Table 5. Analysis of areas selecting for gap junctional plaques\***

	Cell number	Total area ( $\mu\text{m}^2$ )	Median area ( $\mu\text{m}^2$ )	Mean area $\pm$ s.d. ( $\mu\text{m}^2$ )	Median intensity (arbitrary units)	<i>N</i>
Control	70	55.5	0.12	0.28 $\pm$ 0.34	52	201
br-cAMP	69	194.4	0.12	0.30 $\pm$ 0.34	42	651

\*Intensity range of 1-100.

**Table 6. Analysis of areas selecting for cytoplasmic patches\***

	Total area ( $\mu\text{m}^2$ )	Median area ( $\mu\text{m}^2$ )	Mean area $\pm$ s.d. ( $\mu\text{m}^2$ )	Median intensity (arbitrary units)	<i>N</i>
Control	437.8	7.5	10.7 $\pm$ 12.0	179	41
br-cAMP	297.8	6.7	7.6 $\pm$ 3.3	175	39

\*Intensity range of 101 to 200; areas larger than  $\approx 4.3 \mu\text{m}^2$ .

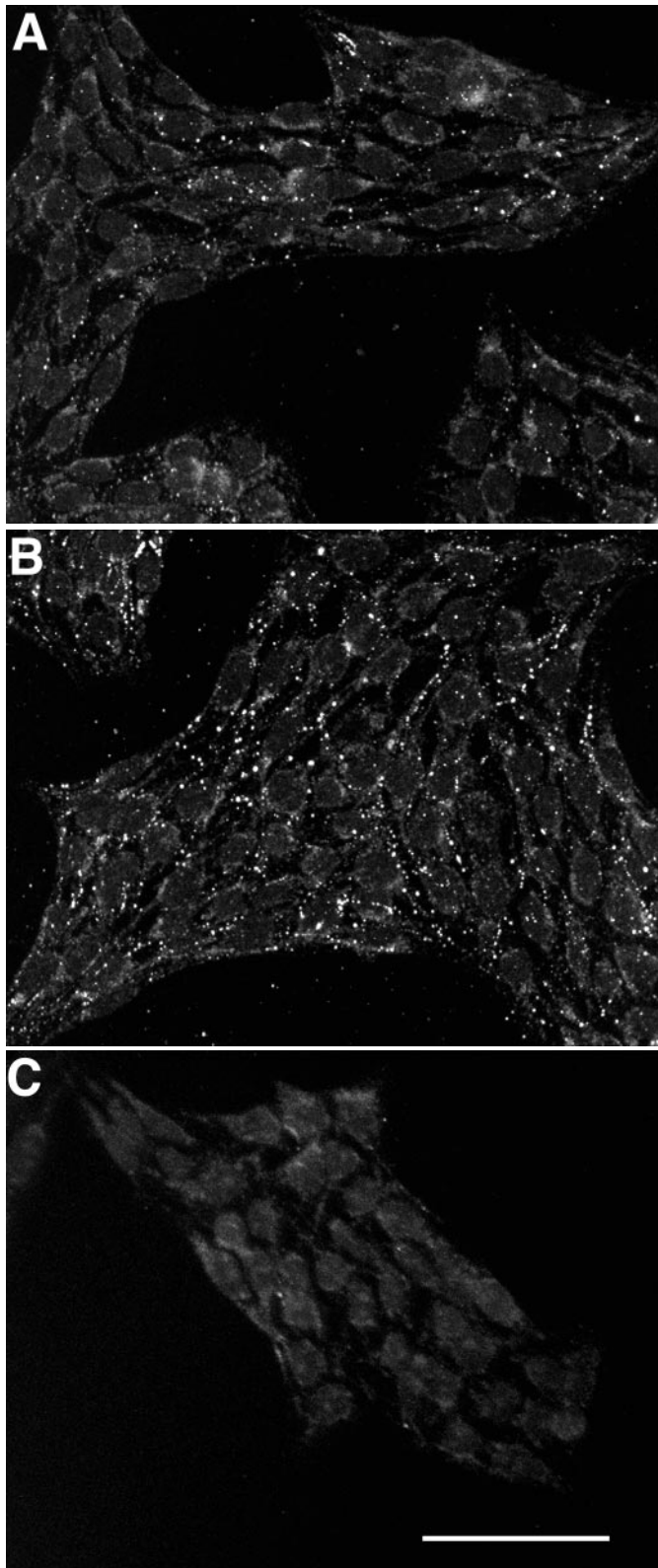


**Fig. 11.** Cx43 immunofluorescence in MMT2 cells without Triton X-100 extraction reveals the distribution of cytoplasmic Cx43. Images are the result of a summation process in which a  $z$ -series is projected two-dimensionally. Optical sections were scanned individually and only the greatest intensity at a given  $x,y$  coordinate was retained for the final image. (A) Control cells. (B) Cells exposed to 300  $\mu$ M br-cAMP for 24 hours. (C) Non-specific staining of cells exposed to the secondary antibody only. Bar, 50  $\mu$ m.

## DISCUSSION

We have used several complementary approaches to characterize the increased gap junctional communication between MMT22 cells brought about by br-cAMP treatment. Three important features emerge from this study: First, an approximately fourfold increase in junctional permeance was accompanied by a proportional fourfold increase in gap junctional plaques and a demonstrated increase in plasma membrane-associated Cx43. These changes occurred without significant changes in Cx43 mRNA or total cellular Cx43. Second, treatment with br-cAMP resulted in an early increase (evident within one hour) in the slower migrating (phosphorylated) species of Cx43. Third, the elevated permeance of the junctional interface and the increase in gap junctions were not attenuated with prolonged exposure to br-cAMP.

We propose that cAMP induces an increase in gap junctional permeance by re-apportioning Cx43 from non-junctional sites to junctional plaques at cell-cell interfaces. The following observations support this conclusion: (1) By quantifying the permeance of cell-cell interfaces and the occurrence of junctional plaques at the interfaces, we were able to show a close correspondence between the two after br-cAMP treatment. These observations suggest that channel number, rather than channel gating, is the salient parameter determining cAMP-induced junctional permeance changes in MMT22 cells. It also should be noted that the time course and longevity of the response to br-cAMP, as shown by permeance measurements and electron microscopy, suggest that something other than gating is involved. That is, gating mechanisms in gap junctional channels typically are manifested more quickly, peak more rapidly, and become attenuated (Bennett et al., 1991), including those mechanisms responsive to cAMP (e.g. Saez et al., 1986). (2) Confocal microscopy of immunofluorescently labeled Cx43, supporting the permeance and electron microscopy data, indicates that Cx43 increased at the plasma membrane with exposure to br-cAMP and appeared to plateau after 24 hours of treatment. (3) The increase in gap junctional channels we observed in MMT22 cells was not due to increased transcription or translation of Cx43 mRNA. Northern blots and western immunoblots showed no consistent change in the amount of Cx43 message or total cellular levels of Cx43 following br-cAMP treatment for periods up to two days. Since the permeance level peaked at 24 hours, the absence of an overall increase in cellular Cx43 during this period indicates that pre-existing Cx43 was recruited for the formation of gap junctions. Consistent changes ( $\approx 50\%$  increases) were obtained in cellular Cx43 protein levels after two days of exposure to br-cAMP. These moderate increases in Cx43 at later times may reflect 'adjustments' in the pool size of Cx43 after new levels of permeance and gap junction development have been established.

However, the total area of these regions was 47% greater in control cells, reflecting the 41% increase in mean area. These results are consistent with the conclusion that Cx43 within cytoplasmic pools is recruited for the formation of an increased number of gap junctions.

This is the only demonstration of which we are aware that indicates cAMP can modify gap junctional permeability through an increased recruitment from cytoplasmic Cx43 stores, and contrasts with other reports. When investigating gap junctional responses to cAMP analogues, two reports have shown severalfold increases in mRNA (Mehta et al., 1992; Schiller et al., 1992). Mehta et al. (1992) have shown that forskolin, an activator of adenylyl cyclase, increased Cx43 mRNA sixfold in a hepatoma cell line, with the increase preceding detectable increases in dye coupling. The large change in Cx43 mRNA was indicated for other cell lines as well. Moreover, the amount of mRNA and dye coupling became refractory with continuous exposure to forskolin or cAMP analogues, and eventually returned to near basal levels. The latter response is also clearly different from that reported here for MMT22 cells, in which high levels of permeance continue unabated for seven days. Our suggestion that increased formation of gap junctions can occur in the absence of increased connexin synthesis does have precedents. Meyer et al. (1991) reported that LDL increased gap junctional formation and dye transfer rates without increasing the total cellular content of Cx43 in suspension cell cultures of a hepatoma cell line. Similarly, De Sousa et al. (1993) reported that *de novo* assembly of gap junctions during compaction of the mouse embryo entails trafficking mechanisms downstream of Cx43 transcription and translation. Also in the latter study, confocal microscopy of the beginning stages of gap junctional formation yielded images with diffuse cytoplasmic Cx43 staining reminiscent of that shown in this report (cf. Fig. 11).

The presence of multiple Cx43 bands obtained in western immunoblots of various cells results from impeded migration of the phosphorylated species (Musil et al., 1990), as has now been well-documented (Brissette et al., 1991; Crow et al., 1990; Laird et al., 1991; Lau et al., 1992; Musil et al., 1990). We confirmed this for MMT22 cells (P. Lampe and M. Atkinson, data not presented) in that cells pre-labeled with  $^{32}\text{P}$ -orthophosphate produced bands in the 44 kDa to 47 kDa range on SDS-PAGE gels following immunoprecipitation of whole cell extracts with Cx43 antibody. No bands were obtained that corresponded to the 41 kDa band on westerns, again consistent with other reports of a non-phosphorylated band of essentially the same size (e.g. Musil et al., 1990). Although densitometric analysis of western immunoblots showed that the total amount of Cx43 changed little over periods of br-cAMP exposure up to seven days, analysis of the individual bands (41 kDa, 44 kDa, and 46 kDa) did show progressive (albeit delayed) increases in the 46 kDa form of Cx43, beginning at 6 hours of br-cAMP exposure. Based on their studies of NRK cell gap junctions, Musil and Goodenough (1991) have proposed that the non-phosphorylated form of Cx43 is converted at the plasma membrane to phosphorylated species in a process that is temporally associated with acquisition of Triton X-100 insolubility and interpreted as insertion into the gap junctional plaque. Our results are in general agreement with this model in that the increase in the 46 kDa form may reflect the observed increase in gap junctional plaques. However, the correlation does not fit particularly well with the permeance data. The increase in the 46 kDa band is only approximately 50% greater than control levels at 24 hours of br-cAMP treatment, a time when the junctional permeance has attained maximal values,

and the levels of the 46 kDa form continue to increase beyond the time at which the junctional permeance has plateaued. Possibly, there is no simple relationship between permeance levels and levels of the 46 kDa Cx43, or perhaps only a portion of the 46 kDa form, not distinguishable on western blots, is the salient species.

A clearer picture emerges when ethanol-fixed MMT cells are detergent-extracted. For these experiments the cells were prepared as for immunofluorescence up to the point of incubation with antibody for immunofluorescence, at which time the detergent-insoluble material remaining on the dish was solubilized with sample buffer for SDS-PAGE. Confocal microscopy of fixed and labeled cells showed that essentially all staining occurred at the periphery of the cells, and that br-cAMP resulted in an increase in this staining (cf. Figs 4,5,6). In agreement with the immunofluorescence data, the amount of total, detergent-insoluble Cx43 in western immunoblots increased over a 24 hour period in the presence of br-cAMP. Since the total amount of Cx43 did not change over this same period (cf. Figs 8,9), br-cAMP treatment resulted in a greater proportion of Cx43 that was at the plasma membrane and resistant to detergent solubilization. All three of the forms of Cx43 characterized in this study were present after ethanol-fixation and detergent-extraction, and the amount of the 41 kDa form did not change in response to br-cAMP. Since most, if not all of the specific staining occurred at the plasma membrane, the results suggest that both phosphorylated and non-phosphorylated forms of Cx43 can be found at the plasma membrane. This does not imply that all forms can be found within the gap junctional plaque (which is detergent-resistant) since the ethanol treatment potentially could affect the detergent solubility of Cx43 in other areas of the plasma membrane. Both the 44 kDa and 46 kDa (phosphorylated) forms of Cx43 showed early increases ( $\approx$ twofold by one hour of br-cAMP treatment) that persisted and usually increased (two- to threefold increases by 24 hours). A comparison of the levels of the 44 kDa form in the absence or presence of detergent shows that while the total amount of this species did not change over time in the presence of br-cAMP, a substantial fraction rapidly acquired and maintained detergent-insolubility in response to br-cAMP. Similarly, there was no change in the amount of the 46 kDa species after a 1 hour exposure to br-cAMP, but an increase of approximately twofold when the detergent-resistant fraction is analyzed. The most straightforward interpretation is that the cellular level of the 46 kDa species did not begin to increase until after 1 hour of br-cAMP treatment, but that more was resistant to detergent by 1 hour. Thus, an early response to br-cAMP may be placement of the 44 kDa form into a detergent-insoluble pool and conversion to the 46 kDa form, akin to the Musil-Goodenough model (Musil and Goodenough, 1991). While these possibilities are consistent with our data, a better understanding of the formation of gap junctions awaits identification of all the possible post-translational modifications of Cx43.

Our observations that the increase in junctional permeability by br-cAMP can be maintained without attenuation suggest that step changes in the levels of cAMP that persist for hours to days would be paralleled by step changes in the level of junctional permeance, and that this would be effected by re-apportioning the amount of Cx43 in non-junctional pools and gap junctions. Such step changes may occur during changes of

cell state such as attainment of a quiescent state (e.g. Flagg-Newton et al., 1981) or further differentiation of a tissue.

We sincerely appreciate and gratefully acknowledge the expert technical assistance of Sig LaVilla. We also acknowledge and thank Dale Laird and Barbara Yancey for providing the connexin43 antibodies, and David Paul for providing the connexin probes. This work was supported by funds from the NIH; CA 30129, CA 51487 and GM 46277.

## REFERENCES

- Atkinson, M. M., Anderson, S. K. and Sheridan, J. D. (1986). Modification of gap junctions in cells transformed by a temperature-sensitive mutant of Rous sarcoma virus. *J. Membr. Biol.* **91**, 53-64.
- Atkinson, M. M. and Sheridan, J. D. (1988). Altered junctional permeability between cells transformed by v-ras, v-mos or v-src. *Am. J. Physiol.* **225**, C674-C683.
- Azarnia, R., Dahl, G. and Loewenstein, W. R. (1981). Cell junctions and cyclic AMP: III. Promotion of junctional membrane permeability and junctional membrane particles in a junction deficient cell type. *J. Membr. Biol.* **63**, 133-146.
- Bennett, M. V. L., Barrio, L. C., Bargiello, T. A., Spray, D. C., Hertzberg, E. and Saez, J. C. (1991). Gap junctions: New tools. New answers. New questions. *Neuron* **6**, 305-320.
- Beyer, E. C. (1993). Gap junctions. *Int. Rev. Cytol.* **137C**, 1-37.
- Biegan, R. P., Atkinson, M. M., Liu, T.-F., Kam, E. Y. and Sheridan, J. D. (1987). Permeance of Novikoff hepatoma gap junctions: Quantitative video analysis of dye transfer. *J. Membr. Biol.* **96**, 225-233.
- Brissette, J. L., Kumar, N. M., Gilula, N. B. and Dotto, G. P. (1991). The tumor promoter 12-O-Tetradecanoylphorbol-13-acetate and the ras oncogene modulate expression and phosphorylation of gap junction proteins. *Mol. Cell. Biol.* **11**, 5364-5371.
- Cho-Chung, Y. S. (1985). The role of cAMP in the control of mammary tumor growth. In *Hormonally Responsive Tumors* (ed. V. P. Hollander), pp. 115-134. Academic Press, Inc. Harcourt Brace Jovanovich, New York.
- Chomczynski, P. and Sacchi, N. (1987). Single-step method of RNA isolation by guanidinium thiocyanate-phenol chloroform extraction. *Anal. Biochem.* **162**, 156-159.
- Crow, D. S., Beyer, E. C., Paul, D. L., Kobe, S. S. and Lau, A. F. (1990). Phosphorylation of connexin43 gap junction protein in uninfected and Rous sarcoma virus-transformed mammalian fibroblasts. *Mol. Cell. Biol.* **10**, 1754-1763.
- De Mello, W. (1984). Effect of intracellular injection of cAMP on the electrical coupling of cardiac cells. *Biochem. Biophys. Res. Commun.* **119**, 1001-1007.
- De Sousa, P. A., Valdimarsson, G., Nicholson, B. J. and Kidder, G. M. (1993). Connexin trafficking and the control of gap junction assembly in mouse preimplantation embryos. *Development* **117**, 1355-67.
- Flagg-Newton, J. L., Dahl, G. and Loewenstein, W. R. (1981). Cell junction and cyclic AMP: I. Upregulation of junctional membrane permeability and junctional membrane particles by administration of cyclic nucleotide or phosphodiesterase inhibitor. *J. Membr. Biol.* **63**, 105-121.
- Keane, R. W., Mehta, P., Rose, B., Honig, L. S., Loewenstein, W. R. and Rutishauser, U. (1988). Neural differentiation, NCAM-mediated adhesion and gap junctional communication in neuroectoderm. A study in vitro. *J. Cell Biol.* **106**, 1307-1319.
- Kiang, D. T., King, M., Zhang, H.-J., Kennedy, B. J. and Wang, N. (1982). Cyclic biological expression in mouse mammary tumors. *Science* **216**, 68-70.
- Laemmli, U. K. (1970). Cleavage of structural proteins during the assembly of the head of bacteriophage T4. *Nature* **227**, 680-685.
- Laird, D. W. and Revel, J. P. (1990). Biochemical and immunochemical analysis of the arrangement of connexin43 in rat heart gap junction membranes. *J. Cell Sci.* **97**, 109-117.
- Laird, D. W., Puranam, K. L. and Revel, J. P. (1991). Turnover and phosphorylation dynamics of connexin43 gap junction protein in cultured cardiac myocytes. *Biochem. J.* **273**, 67-72.
- Lampe, P. D. and Johnson, R. G. (1990). Amino acid sequence of in vivo phosphorylation sites in the main intrinsic protein (MIP) of lens membranes. *Eur. J. Biochem.* **194**, 541-547.
- Lau, A. F., Kanemitsu, M. Y., Kurata, W. E., Danesh, S. and Boynton, A. L. (1992). Epidermal growth factor disrupts gap-junctional communication and induces phosphorylation of connexin43 on serine. *Mol. Biol. Cell* **3**, 865-874.
- Loewenstein, W. R. (1990). Cell-to-cell communication and the control of growth. *Am. Rev. Respir. Dis.* **142**, S48-S53.
- Loewenstein, W. R. and Rose, B. (1992). The cell-cell channel in the control of growth. *Semin. Cell Biol.* **3**, 59-79.
- Mehta, P. P., Yamamoto, M. and Rose, B. (1992). Transcription of the gene for the gap junctional protein connexin43 and expression of functional cell-to-cell channels are regulated by cAMP. *Mol. Biol. Cell* **3**, 839-50.
- Meyer, R. A., Lampe, P. D., Malewicz, B., Baumann, W. and Johnson, R. G. (1991). Enhanced gap junction formation with LDL and apolipoprotein B. *Exp. Cell Res.* **196**, 72-81.
- Meyer, R. A., Laird, D. W., Revel, J.-P. and Johnson, R. G. (1992). Inhibition of gap junction and adherens junction assembly by connexin and A-CAM antibodies. *J. Cell Biol.* **119**, 179-189.
- Murray, S. A. and Taylor, F. (1988). Dibutyryl cyclic AMP modulation of gap junctions in SW-13 human adrenal cortical tumor cells. *Am. J. Anat.* **181**, 141-8.
- Musil, L. S., Beyer, E. C. and Goodenough, D. A. (1990a). Expression of the gap junction protein connexin43 in embryonic chick lens: Molecular cloning, ultrastructural localization, and post-translational phosphorylation. *J. Membr. Biol.* **116**, 163-175.
- Musil, L. S., Cunningham, B. A., Edelman, G. M. and Goodenough, D. A. (1990b). Differential phosphorylation of gap junction protein connexin43 in junctional communication-competent and -deficient cell lines. *J. Cell Biol.* **111**, 2077-2088.
- Musil, L. S. and Goodenough, D. A. (1991). Biochemical analysis of connexin43 intracellular transport, phosphorylation and assembly into gap junctional plaques. *J. Cell Biol.* **115**, 1357-1374.
- Musil, L. S. and Goodenough, D. A. (1993). Multisubunit assembly of an integral plasma membrane channel protein, gap junction connexin43, occurs after exit from the ER. *Cell* **74**, 1065-77.
- Preus, D., Johnson, R. and Sheridan, J. (1981). Gap junctions between Novikoff hepatoma cells following dissociation and recovery in the absence of cell contact. *J. Ultrastruct. Res.* **77**, 248-262.
- Saez, J. C., Spray, D. C., Nairn, A. C., Hertzberg, E., Greengard, P. and Bennett, M. V. L. (1986). cAMP increases junctional conductance and stimulates phosphorylation of the 27-kDa principle gap junction polypeptide. *Proc. Nat. Acad. Sci. USA* **83**, 2473-2477.
- Saez, J. C., Gregory, W. A., Watanabe, T., Dermietzel, R., Hertzberg, E. L., Reid, L. R., Bennett, M. V. L. and Spray, D. C. (1989). cAMP delays disappearance of gap junctions between pairs of rat hepatocytes in primary culture. *Am. J. Physiol.* **257**, C1-C11.
- Schiller, P. C., Mehta, P. P., Roos, B. A. and Howard, G. A. (1992). Hormonal regulation of intercellular communication: parathyroid hormone increases connexin 43 gene expression and gap-junctional communication in osteoblastic cells. *Mol. Endocrinol.* **6**, 1433-40.
- Sheridan, J. D. (1987). Cell communication and growth. In *Cell-to-Cell Communication* (ed. W. C. d. Mello), pp. 187-222. Plenum Press, Inc., New York.
- Trosko, J. E., Chang, C. C., Madhukar, B. V. and Klaunig, J. E. (1990). Chemical, oncogene, and growth factor inhibition of gap junctional intercellular communication: an integrative hypothesis of carcinogenesis. *Pathobiology* **58**, 265-278.
- Yancey, S. B., John, S. A., Lal, R., Austin, B. J. and Revel, J. P. (1989). The 43-kD polypeptide of heart gap junctions: Immunolocalization (I), topology (II), and functional domains (III). *J. Cell Biol.* **108**, 2241-2254.

(Received 14 February 1995 - Accepted 15 June 1995)